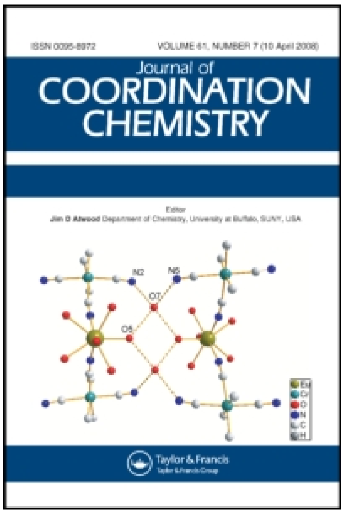

Journal of Coordination Chemistry
Publication details, including instructions for authors and subscription information:
http://www.informaworld.com/smpp/title~content=t713455674

High-spin complexes of iron(III) with ethylene glycol and 3(2'-hydroxyphenyl)-5-(4'-substituted phenyl) pyrazolines

U. N. Tripathi[a]; Afshan Siddiqui[a]; Mohd. Safi Ahmad[b]; Kajal Singh[a]
[a] Department of Chemistry, DDU Gorakhpur University, Gorakhpur 273001, Uttar Pradesh, India [b] School of Studies in Chemistry, Vikram University, Ujjain 456010, Madhya Pradesh, India

First published on: 23 February 2010

To cite this Article Tripathi, U. N. , Siddiqui, Afshan , Ahmad, Mohd. Safi and Singh, Kajal(2010) 'High-spin complexes of iron(III) with ethylene glycol and 3(2'-hydroxyphenyl)-5-(4'-substituted phenyl) pyrazolines', Journal of Coordination Chemistry, 63: 5, 894 — 905, First published on: 23 February 2010 (iFirst)

To link to this Article: DOI: 10.1080/00958971003645920

URL: http://dx.doi.org/10.1080/00958971003645920

Journal of Coordination Chemistry
Vol. 63, No. 5, 10 March 2010, 894–905

Taylor & Francis
Taylor & Francis Group

High-spin complexes of iron(III) with ethylene glycol and 3(2′-hydroxyphenyl)-5-(4′-substituted phenyl) pyrazolines

U.N. TRIPATHI*†, AFSHAN SIDDIQUI†, MOHD. SAFI AHMAD‡
and KAJAL SINGH†

†Department of Chemistry, DDU Gorakhpur University, Gorakhpur 273001,
Uttar Pradesh, India
‡School of Studies in Chemistry, Vikram University, Ujjain 456010,
Madhya Pradesh, India

(*Received 9 June 2009; in final form 12 October 2009*)

Complexes of iron(III) with ethylene glycol and 3(2′-hydroxyphenyl)-5-(4′-substituted phenyl) pyrazolines, $[Fe(OCH_2CH_2O)(C_{15}H_{12}N_2OX)]_m \cdot nH_2O$ and $[Fe(C_{15}H_{12}N_2OX)_2(OCH_2CH_2OH)]$ (where OCH_2CH_2O and OCH_2CH_2OH = ethylene glycol moiety; $C_{15}H_{12}N_2OX$ = 3(2′-hydroxyphenyl)-5-(4-X-phenyl)pyrazoline; X = H, CH_3, OCH_3, or Cl; $m = 2–3$ and $n = 2–3$) have been synthesized and characterized by elemental analysis (C, H, N, Cl, and Fe), molecular weight measurement, magnetic moment data, thermogravimetric analysis, molar conductance, spectral (UV-Vis, IR, and FAB mass), scanning electron microscopy, and X-ray diffraction studies. Bonding of ethylene glycol and pyrazolines in these complexes and the particle size of iron(III) complexes are discussed. Antibacterial and antifungal potential of free pyrazoline and some iron(III) complexes are also discussed.

Keywords: Iron(III); Pyrazolinates; Ethylene glycolate; Antimicrobial activity; High-spin complexes

1. Introduction

Coordination chemistry of pyrazolines and their derivatives have wide applicability. Pyrazolines are an important class of heterocyclic compounds used in industries as dyes, lubricating oils, antioxidants, and in agriculture as catalysts for decarboxylation, as well as inhibitors for plant growth [1–3]. Complexation behavior of 3(2′-hydroxyphenyl)-5-phenylpyrazoline with Ni(II), Co(II), and Cu(II) have been investigated in our laboratories [4]. We have also investigated the complexation behavior and antimicrobial potential of 3(2′-hydroxyphenyl)-5-phenylpyrazoline and substituted pyrazolines with tin(IV), organotin(IV), diorganotin(IV), and triorganotin(IV) [5–9]. We have also studied the synthesis, spectra, and antimicrobial activity of dichloroantimony(III)

---

*Corresponding author. Email: un_tripathi@yahoo.com

Journal of Coordination Chemistry
ISSN 0095-8972 print/ISSN 1029-0389 online
DOI: 10.1080/00958971003645920

pyrazolinates, chloroantimony(III) dipyrazolinates, dichlorobismuth(III) pyrazolinates, and chlorobismuth(III) dipyrazolinates [10, 11].

Iron is the most important transition element in living systems, vital to both plants and animals. Iron plays crucial roles in the transport and storage of oxygen and also in electron transport. Ethylene glycol complexes of iron(II) were first prepared by Gomer and Tyson [12]. Later, Knetsch and Groeneveld [13, 14] reported the preparation of the well-defined iron(II) ethylene glycol complexes. The final characterization of iron(II) ethylene glycol complexes by means of temperature-dependent magnetic susceptibility and Mossbauer spectroscopic measurements was reported by Labadi *et al.* [15].

In continuation to our previous work, we study the complexation behavior of 3(2′-hydroxyphenyl)-5-phenyl pyrazoline and substituted pyrazoline with iron(III). We have studied the synthesis, spectral study, and antimicrobial activity of iron(III) 5(2′-hydroxyphenyl)-3-(4′-substituted phenyl) pyrazolinates and their addition complexes with N, P donor ligands [16]. In this article, we describe the synthesis, characterization, and *in vitro* antimicrobial activity of mixed-ligand complexes of iron(III) with ethylene glycol and 3(2′-hydroxyphenyl)-5-(4′-substituted phenyl) pyrazolines.

2. Experimental

2.1. *Materials and methods*

Solvents (benzene, isopropanol, and ethanol) were rigorously dried and purified by standard methods before use [17]. All chemicals were of analytical grade quality. Ferric chloride (E. Merck), ethylene glycol (BDH), sodium metal (SD fine), *o*-hydroxyacetophenone (CDH), and benzaldehydes (E. Merck) were used as received. Pyrazolines were prepared by the reported procedure [18].

2.2. *Synthesis of $[Fe(OCH_2CH_2O)(C_{15}H_{12}N_2OX)]_m\cdot nH_2O$*

The mixed ligand iron(III) complexes, $[Fe(OCH_2CH_2O)(C_{15}H_{12}N_2OX)]_m\cdot nH_2O$, were prepared by the following two steps:

$$FeCl_3 + Na_2(OCH_2CH_2O) \rightarrow FeCl(OCH_2CH_2O) + 2\ NaCl$$

$$FeCl(OCH_2CH_2O) + Na(C_{15}H_{13}N_2OX) \rightarrow [Fe(OCH_2CH_2O)(C_{15}H_{12}N_2OX)]_m\cdot nH_2O + NaCl$$

(where X = H, CH_3, OCH_3, or Cl; $m = 2$–3; $n = 2$–3).

2.3. *Synthesis of $[Fe(OCH_2CH_2O)(C_{15}H_{12}N_2OCl)]_2\cdot 2H_2O$*

Freshly cut pieces of sodium (0.39 g, 16.95 mM) were taken in a flask with excess isopropanol and refluxed for ~30 min until a clear solution of sodium isopropoxide was obtained. Ethylene glycol (0.53 g, 8.54 mM) was then added and the reaction mixture was further refluxed for ~1 h, giving a yellow solution. The reaction mixture was cooled to room temperature and then ethanolic solution of anhydrous iron(III) chloride (1.38 g, 8.51 mM) was added dropwise with constant stirring. The reaction mixture was further stirred for 2–4 h under reflux until the reaction mixture changed from yellow to brown–black. The reaction mixture was filtered at 40–45°C through alkoxy funnel under vacuum to separate the solid sodium chloride. The clear filtrate was used in the next step.

Freshly cut pieces of sodium (0.19 g, 8.26 mM) were taken in a flask with excess isopropanol and refluxed for ~30 min until a clear solution of sodium isopropoxide was obtained. The solution of 3(2′-hydroxyphenyl)-5(4′-chlorophenyl) pyrazoline (2.19 g, 8.03 mM) in anhydrous ethanol was then added and the reaction mixture was further refluxed for ~1 h, giving a yellow solution. The reaction mixture containing sodium salt of pyrazoline was cooled to room temperature and added dropwise to the above filtrate [containing iron(III) complex of ethylene glycol] with constant stirring. The reaction mixture was further stirred for 2–4 h. The reddish brown to black solid so obtained was filtered and repeatedly washed with hot water to remove sodium chloride. The solid was finally washed with isopropanol and dried at 80°C, and 5.00 g of $[Fe(OCH_2CH_2O)(C_{15}H_{12}N_2OCl)]_2 \cdot 2H_2O$ was obtained. Compounds **1**–**3** were prepared by the same method. The analytical details are summarized in table 1.

2.4. *Synthesis of* $[Fe(C_{15}H_{12}N_2OX)_2(OCH_2CH_2OH)]$

Iron(III) complex, $[Fe(C_{15}H_{12}N_2OX)_2(OCH_2CH_2OH)]$, is prepared by the following two steps:

$$FeCl_3 + 2Na(C_{15}H_{12}N_2OX) \rightarrow FeCl(C_{15}H_{12}N_2OX)_2 + 2NaCl$$

$$FeCl(C_{15}H_{12}N_2OX)_2 + HOCH_2CH_2OH \rightarrow [Fe(C_{15}H_{12}N_2OX)_2(OCH_2CH_2OH)] + HCl$$

(where X = H, CH_3, OCH_3, or Cl).

2.5. *Synthesis of* $[Fe(C_{15}H_{12}N_2OCl)_2(OCH_2CH_2OH)]$

Freshly cut pieces of sodium (0.19 g, 8.26 mM) were taken in a flask with excess isopropanol and refluxed for ~30 min until a clear solution of sodium isopropoxide was obtained. The solution of 3(2′-hydroxyphenyl)-5(4′-chlorophenyl) pyrazoline (2.25 g, 8.25 mM) in anhydrous ethanol was then added and the reaction mixture was further refluxed for ~1 h, giving a yellow solution. The reaction mixture was cooled to room temperature and ethanolic solution of anhydrous iron(III) chloride (0.67 g, 4.13 mM) was added dropwise with constant stirring. The reaction mixture was stirred for 2–4 h under reflux until the mixture changed from yellow to reddish brown and was filtered through an alkoxy funnel under vacuum to separate the solid compound, which was washed with hot water to remove sodium chloride and finally with isopropanol. The solid so obtained was dried at 80°C.

The solid obtained above was dissolved in benzene. To the above benzene solution, ethylene glycol (0.25 g, 4.03 mM) and a few drops of triethylamine were added.

Table 1. Physical and analytical data for [Fe(OCH_2CH_2O)($C_{15}H_{12}N_2OX$)]$_m$·$n$$H_2O$ and [Fe($C_{15}H_{12}N_2OX$)$_2$(OCH_2CH_2OH)].

				Analysis found (Calcd) (in %)					
Compound No.	Compound	Yield (%)	m.p. (°C)	C	H	N	Cl	Fe	Molecular weight found (Calcd)
1	[Fe(OCH_2CH_2O)($C_{15}H_{12}N_2OX$)]$_3$·$3H_2O$	68	178	55.15 (55.01)	5.13 (5.16)	7.51 (7.55)	–	15.10 (15.05)	1113 (1113.57)
2	[Fe(OCH_2CH_2O)($C_{15}H_{12}N_2OX$)]$_2$·$2H_2O$	79	225	56.16 (56.12)	5.51 (5.49)	7.32 (7.27)	–	14.43 (14.50)	770 (770.43)
3	[Fe(OCH_2CH_2O)($C_{15}H_{12}N_2OX$)]$_2$·$2H_2O$	77	240	53.78 (53.88)	5.26 (5.28)	6.97 (6.98)	–	13.86 (13.92)	802 (802.43)
4	[Fe(OCH_2CH_2O)($C_{15}H_{12}N_2OX$)]$_2$·$2H_2O$	75	200	50.25 (50.34)	4.49 (4.47)	6.95 (6.91)	8.78 (8.74)	13.82 (13.77)	811 (811.27)
5	[Fe($C_{15}H_{12}N_2OX$)$_2$(OCH_2CH_2OH)]	89	200	64.99 (64.98)	5.30 (5.28)	9.51 (9.47)	–	9.48 (9.44)	591 (591.16)
6	[Fe($C_{15}H_{12}N_2OX$)$_2$(OCH_2CH_2OH)]	88	225	65.88 (65.92)	5.66 (5.69)	9.06 (9.04)	–	9.22 (9.01)	619 (619.51)
7	[Fe($C_{15}H_{12}N_2OX$)$_2$(OCH_2CH_2OH)]	91	250	62.77 (62.68)	5.45 (5.41)	8.55 (8.60)	–	8.59 (8.57)	651 (651.51)
8	[Fe($C_{15}H_{12}N_2OX$)$_2$(OCH_2CH_2OH)]	90	210	58.26 (58.20)	4.41 (4.43)	8.44 (8.48)	10.81 (10.74)	8.48 (8.46)	660 (660.35)

X = H in **1** and **5**; CH_3 in **2** and **6**; OCH_3 in **3** and **7**; and Cl in **4** and **8**.

The reaction mixture was stirred for 6–8 h under reflux and then filtered at 40–45°C through an alkoxy funnel under vacuum to separate the solid sodium chloride. The solvents were removed from the filtrate under vacuum giving reddish-brown to black solid. The solid so obtained was repeatedly washed with hot water to remove sodium chloride. The solid was finally washed with isopropanol and dried at 80°C. 2.40 g of $[Fe(C_{15}H_{12}N_2OCl)_2(OCH_2CH_2OH)]$ was obtained. Compounds **5**–**7** were prepared by the same method. The analytical details are summarized in table 1.

2.6. *Physical measurements*

Chlorine was estimated by Volhard's method [17] and iron was determined gravimetrically as ferric oxide [19]. The melting points (°C) of the compounds were recorded on a BI Barnstead electrothermal instrument. Molecular weights were determined on a Knauer Vapour pressure osmometer in $CHCl_3$ at 45°C. Elemental analyses (C, H, and N) were obtained using a Coleman CHN analyzer. Magnetic moment studies were carried out on a Gouy balance at room temperature. Infrared spectra were recorded as Nujol mulls using CsI cells on a Perkin-Elmer Model 557 FT-IR spectrophotometer from 4000 to 200 cm^{-1}. FAB mass spectra were recorded on a JEOL SX 102/DA-6000 mass spectrometer. Electronic spectra were recorded in benzene solution on a Hitachi U-2000 UV-Vis spectrophotometer. Thermogravimetric analysis (TGA) was carried out at a heating rate of 5 min^{-1} using an instrument with Rigaku Thermoflex PTC-10A processor supplied by USIC, Delhi University, New Delhi, India. The molar conductivities of the ligand and complexes were determined in DMF (1.0×10^{-3} M) at room temperature using a Metrohm 712 conductometer. The X-ray diffraction (XRD) studies were carried out on a Bruker Nonius Kappa CCD diffractometer at room temperature. Scanning electron microscopy (SEM) images were recorded with a ZEISS EVO microscope operating at 20 kV. The specific optical rotations were recorded at 25°C in benzene on a Perkin-Elmer polarimeter (model 341) using the sodium D line ($\lambda = 589$ nm).

2.7. *Antimicrobial studies*

Agar disc diffusion was used for the screening of *in vitro* antimicrobial activity [20]. Inocula of bacteria were prepared in nutrient broth and fungi in potato dextrose agar slant. The cultures were inoculated and incubated for 48 h in case of bacteria and for 5 days in case of fungi. The molten Mueller–Hinton medium was poured in sterile petri dishes (9 cm in diameter) to get a depth of 5 mm. The medium was left to solidify. Thereafter, it was seeded with respective test organisms. For the purpose of seeding, 5 mL sterile water was added to agar slant culture of fungi. The culture was scraped to get a suspension of fungi spore. A sterile cotton swab was dipped in the culture/suspension and lightly rubbed over the solidified medium. The plate was left for few minutes and then used for the test. 30 µm of each sample to be tested were dissolved in 1 mL of acetone. 5 mm discs of Whatman filter paper no. 42 were cut and sterilized. The filter paper discs were immersed in solution of sample, removed and left in a sterile petri dish to permit the solvent to evaporate. After 10 min, the paper discs were transferred to seeded agar plate and incubated at 37°C for 24 h (for bacteria) and at 30°C for 72 h (for fungi), where inhibition zones were detected around each disc.

A disc soaked in acetone alone was used as a control under the same conditions and there was no observed inhibition zone for acetone. Diameter of each distinct inhibition zone was measured in millimeter, both antibacterial and antifungal activity can be calculated as a mean of three replica.

3. Results and discussion

$[Fe(OCH_2CH_2O)(C_{15}H_{12}N_2OX)]_m \cdot nH_2O$ and $[Fe(C_{15}H_{12}N_2OX)_2(OCH_2CH_2OH)]$ are reddish brown to black solids, non-hygroscopic, stable at room temperature, and soluble in common organic (benzene, chloroform, and acetone) and coordinating (tetrahydrofuran, dimethylformamide, and dimethylsulfoxide) solvents at slightly elevated temperature. Molecular weight measurements in dilute chloroform at 45°C show monomeric $[Fe(C_{15}H_{12}N_2OX)_2(OCH_2CH_2OH)]$ complexes. $[Fe(OCH_2CH_2O)(C_{15}H_{12}N_2OX)]_m \cdot nH_2O$ with $X = H$ is trimeric, while complexes with $X = CH_3$, OCH_3, and Cl are dimeric. The elemental analysis (C, H, N, Cl, and Fe) data are in accord with stoichiometry proposed (table 1).

3.1. *Specific optical rotation data*

The specific optical rotation values of benzene solution of free pyrazolines and mixed ligand complexes of iron(III) are not measurable at the concentration of 1.00%, 0.50%, 0.10%, and 0.05% due to the dark color of solution. All four pyrazolines show zero specific optical rotation at 0.02% concentration. Thus, free pyrazolines are racemic mixture. The specific optical rotation values for iron(III) complexes in benzene solution at 0.02% concentration are also zero, indicating that these iron(III) complexes exist as racemic mixture.

3.2. *Magnetic moment data*

The magnetic moment data are summarized in table 2. The effective magnetic moment (μ_{eff}) values for these compounds range from 5.20 to 5.90 BM, clearly indicating that these iron(III) complexes are high-spin paramagnetic. The oligomeric nature of some complexes reduces the distance between metal centers and leads to sizable antiferromagnetic interaction. Thus, magnetic moments obtained for these complexes are less than the expected value for free metal ions.

3.3. *Molar conductance*

The molar conductances of these iron(III) complexes are 9.10–21.50 $Ohm^{-1}\,cm^2\,M^{-1}$ in DMF (10^{-3} M) solution, too low to account for electrolytic behavior.

Table 2. Electronic spectral and magnetic moment data for **1–8**.

Compound No.	Electronic spectral band			Magnetic moment (BM)
	Assignment	Band (cm^{-1})	Extinction coefficients	
1	$d \rightarrow d$	9993	987	5.90
	$d \rightarrow \pi^*$	31,843	896	
	$n \rightarrow \pi^*$, $\pi \rightarrow \pi^*$	46,430	166	
2	$d \rightarrow d$	9989	980	5.45
	$d \rightarrow \pi^*$	31,926	902	
	$n \rightarrow \pi^*$, $\pi \rightarrow \pi^*$	46,428	170	
3	$d \rightarrow d$	10,025	979	5.40
	$d \rightarrow \pi^*$	32,195	890	
	$n \rightarrow \pi^*$, $\pi \rightarrow \pi^*$	46,432	162	
4	$d \rightarrow d$	10,030	985	5.30
	$d \rightarrow \pi^*$	31,876	905	
	$n \rightarrow \pi^*$, $\pi \rightarrow \pi^*$	46,254	175	
5	$^6A_{1g} \rightarrow {}^4T_{1g}$	18,020	1200	5.20
	$d \rightarrow \pi^*$	32,258	990	
	$n \rightarrow \pi^*$, $\pi \rightarrow \pi^*$	46,424	827	
6	$^6A_{1g} \rightarrow {}^4T_{1g}$	18,358	1195	5.35
	$d \rightarrow \pi^*$	32,400	998	
	$n \rightarrow \pi^*$, $\pi \rightarrow \pi^*$	46,430	830	
7	$^6A_{1g} \rightarrow {}^4T_{1g}$	18,120	1208	5.30
	$d \rightarrow \pi^*$	32,450	1010	
	$n \rightarrow \pi^*$, $\pi \rightarrow \pi^*$	46,426	820	
8	$^6A_{1g} \rightarrow {}^4T_{1g}$	18,050	1203	5.48
	$d \rightarrow \pi^*$	32,520	105	
	$n \rightarrow \pi^*$, $\pi \rightarrow \pi^*$	46,252	815	

3.4. *Thermogravimetric analysis*

The thermograms have been recorded for $[Fe(OCH_2CH_2O)(C_{15}H_{12}N_2OX)]_m \cdot nH_2O$ from 0 to 600°C to insure involvement of water in coordination (table 3).

All four iron(III) complexes of the type $[Fe(OCH_2CH_2O)(C_{15}H_{12}N_2OX)]_m \cdot nH_2O$ show decomposition. Weight loss of 4.8% at 184°C in **1** corresponds to the loss of three coordinated waters. Similarly, weight losses of 4.4–4.6% at 173–181°C in **2–4** correspond to the loss of two coordinated waters. The presence of water is also supported by IR spectral data. All complexes give ferric oxide at ~490°C.

3.5. *UV-Vis spectra*

Electronic absorption spectral data of $[Fe(C_{15}H_{12}N_2OX)_2(OCH_2CH_2OH)]$ in benzene, summarized in table 2, show absorptions in the regions 18,020–18,358, 32,258–32,520, and 46,252–46,430 cm^{-1}. Bands in the region 18,020–18,358 cm^{-1} are characteristic of octahedral geometry and may be assigned to $d \rightarrow d$ transitions arising from the $^6A_{1g} \rightarrow {}^4T_{1g}$ transition. Bands in the region 32,258–32,520 cm^{-1} may be assigned to metal-to-ligand charge transfer transitions arising from the $d \rightarrow \pi^*$ transition and bands in the region 46,252–46,430 cm^{-1} can be assigned to intraligand, $\pi \rightarrow \pi^*$ and $n \rightarrow \pi^*$ transitions of the pyrazoline [16, 21–23].

Electronic absorption spectra of $[Fe(OCH_2CH_2O)(C_{15}H_{12}N_2OX)]_m \cdot nH_2O$ in benzene show absorptions in the regions 9989–10,030, 31,843–32,195, and

Table 3. TGA data for $[Fe(OCH_2CH_2O)(C_{15}H_{12}N_2OX)]_m{\cdot}nH_2O$.

		Theoretical value		Observed value		
Compound No.	Temperature (°C)	Weight loss (%)	Residual mass	Weight loss (%)	Residual mass (mg)[a]	Weight loss between two steps
1	184	4.80	1060.12	4.80	4.28	4.80
	285	21.50	874.15	21.50	3.53	16.70
	490	85.60	160.35	85.60	0.65	64.10
2	181	4.60	734.99	4.67	4.29	4.60
	243	20.70	610.95	20.67	3.57	16.00
	475	86.20	106.32	86.20	0.62	65.50
3	173	4.40	767.12	4.40	4.30	4.40
	235	19.80	643.55	19.80	3.61	15.40
	486	86.60	107.52	86.60	0.60	66.80
4	178	4.40	775.57	4.40	4.30	4.40
	270	19.70	651.45	19.90	3.60	15.30
	479	86.90	106.27	86.90	0.59	67.20

[a] TGA analysis was carried out with 4.50 mg of the respective compounds.

46,254–46,432 cm^{-1}. Bands in the region 9989–10,030 cm^{-1} are consistent with five-coordinate square pyramidal iron(III) complexes, assigned to d → d transitions [24, 25]. Further assignment of absorption bands is difficult due to the interactions of metal–ligand π-systems. Absorptions in the region 31,843–32,195 cm^{-1} may be assigned to metal-to-ligand charge transfer transitions arising from the $d \rightarrow \pi^*$ and bands in the region 46,254–46,432 cm^{-1} can be assigned to intraligand, $\pi \rightarrow \pi^*$ and $n \rightarrow \pi^*$ transitions of the pyrazoline [16, 22].

3.6. *IR spectral data*

The infrared spectral data of these iron(III) complexes (Supplementary material) show bands in the regions 3382–3368, 1630–1608, 593–567[1], and 484–462 cm^{-1} which are assigned to ν(N–H), ν(C=N), ν(Fe–O), and ν(Fe–N), respectively [5–11, 16, 21, 22, 25–27]. Bands in the IR spectra of these iron(III) complexes are consistent with IR spectra of iron(III) pyrazolinates [16]. Thus, pyrazoline is bidentate in these iron(III) complexes.

Two new bands in IR spectra of these iron(III) complexes (in comparison to iron(III) pyrazolinates) [16] in the regions 1018–1008 and 611–599 cm^{-1} may be assigned to ν(C–O) and ν(Fe–O), respectively [16, 21, 22, 25–27]. These bands clearly indicate coordinated ethylene glycol.

A broad band for $[Fe(OCH_2CH_2O)(C_{15}H_{12}N_2OX)]_m \cdot nH_2O$ (in comparison to iron(III) pyrazolinates) [16] at 3425–3405 cm^{-1} is assigned to ν(O–H). The appearance of ν(O–H) suggests the presence of water in $[Fe(OCH_2CH_2OH)(C_{15}H_{12}N_2OX)]_m \cdot nH_2O$ and confirms the TGA data. A sharp band of medium intensity for $[Fe(C_{15}H_{12}N_2OX)_2(OCH_2CH_2OH)]$ at 3630–3622 cm^{-1} is assigned to ν(O–H), suggesting the presence of hydroxyl in the complexes and could be from ethylene glycol.

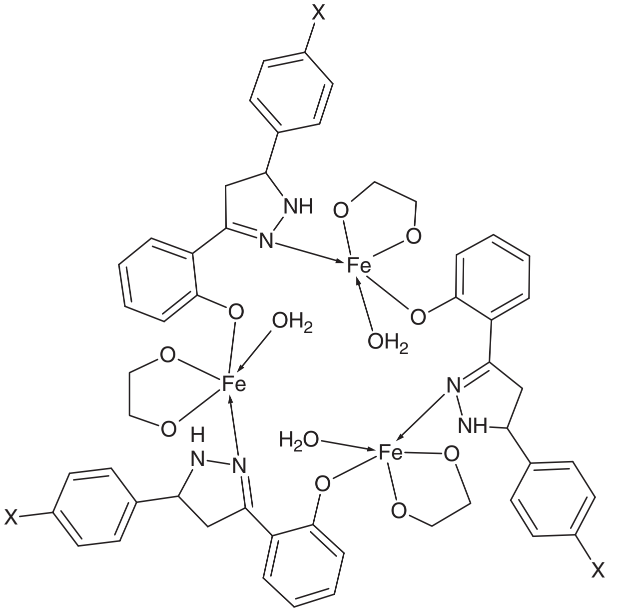

Figure 1. Molecular structure of $[Fe(C_2H_4O_2)(C_{15}H_{12}N_2OX)]_3 \cdot 3H_2O$ (where X = H).

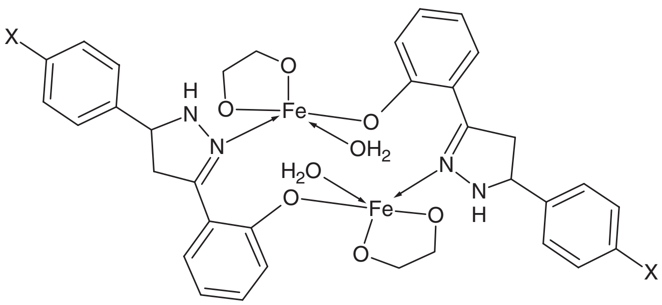

Figure 2. Molecular structure of $[Fe(C_2H_4O_2)(C_{15}H_{12}N_2OX)]_2 \cdot 2H_2O$ (where X = CH_3, OCH_3, and Cl).

3.7. *FAB mass spectra*

The FAB mass spectra for $[Fe(OCH_2CH_2O)(C_{15}H_{12}N_2OX)]_3 \cdot 3H_2O$ (where X = H), $[Fe(OCH_2CH_2O)(C_{15}H_{12}N_2OX)]_2 \cdot 2H_2O$ (where X = OCH_3], and $[Fe(C_{15}H_{12}N_2OX)_2(OCH_2CH_2OH)]$ (where X = H) confirm the molecular weight of the complexes, determined by Knauer Vapour pressure osmometer. The molecular ion peak at $m/z = 1113$ in the FAB mass spectrum of 1 confirms its existence as trimer. Similarly, the dimeric 3 and monomeric 5 are clearly indicated by their respective molecular ion peaks. The fragmentation of 3 is depicted in "Supplementary material". On the basis of the above discussion and available literature, the most plausible geometries around iron(III) in $[Fe(OCH_2CH_2O)(C_{15}H_{12}N_2OX)]_m \cdot nH_2O$ and $[Fe(C_{15}H_{12}N_2OX)_2(OCH_2CH_2OH)]$ are shown in figures 1–3.

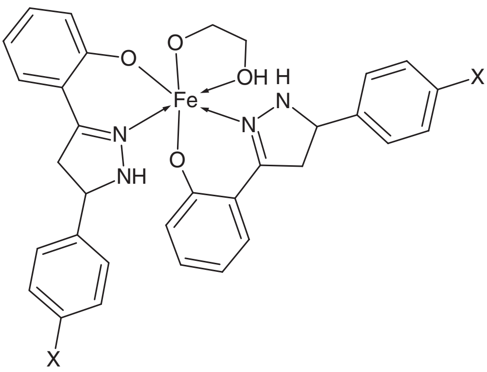

Figure 3. Molecular structure of $[Fe(C_{15}H_{12}N_2OX)_2(C_2H_5O_2)]$ (where $X = H$, CH_3, OCH_3, and Cl).

3.8. *XRD and SEM studies*

The complexes are amorphous solids through XRD; all the complexes. The morphology of the iron(III) complexes were studied by XRD and SEM. The mean diameter of the different particles synthesized are summarized in Supplementary material as are SEM image of $[Fe(OCH_2CH_2O)(C_{15}H_{12}N_2OX)]_2 \cdot 2H_2O$ (where $X = CH_3$) and XRD micrograph of $[Fe(OCH_2CH_2O)(C_{15}H_{12}N_2OX)]_2 \cdot 2H_2O$ (where $X = OCH_3$). The particle size measured from XRD are near to nanoparticle size. However, SEM images show large size for these particles. Large size can be explained by intermolecular hydrogen bonding resulting in associated molecules of large particle size.

3.9. *Microbial assay*

The antibacterial activities of free ligand and two complexes were tested against *Staphylococcus aureus*, *Bacillus licheniformis*, *Escherichia coli*, *Pseudomonas aeruginosa*, *Salmonella typhi*, *Citrobacter freundii*, *Vibrio parahaemolyticus*, and *Candida albicans* and the antifungal activities were tested against *Aspergillus niger* and *Penicillium notatum*. The antimicrobial activity of some antibiotics were also tested and compared with free pyrazoline, and mixed ligand iron(III) complexes. The results are listed in table 4.

Antimicrobial activities of the free pyrazoline and iron(III) complexes with known antibiotics exhibit the following results: (1) The complexes exhibit greater antibacterial effect toward *S. aureus* than free pyrazoline and chloramphenicol. (2) The complexes exhibit greater antibacterial effect toward *P. aeruginosa* than free pyrazoline and chloramphenicol. (3) The complexes exhibit comparable effect toward *B. licheniformis*, *S. typhi*, and *C. albicans* than free pyrazoline and chloramphenicol. (4) The complexes exhibit greater antifungal effect toward *A. niger* and *P. notatum* than free pyrazoline and terbinafin. It is difficult to make a structure and activity relationship between antimicrobial activity and the structures of these complexes, but the complexation of iron(III) with biologically active pyrazoline ligand results in increased activity. Correlation between geometry around central atom in a complex and antimicrobial activity of the same complex is a further area of research.

Table 4. Antimicrobial activity of the free pyrazoline (**1** and **5**).

	Fungi		Gram (+ve) bacteria		Gram (–ve) bacteria		
S. No.	*A. niger*	*P. notatum*	*S. aureus*	*B. licheniformis*	*P. aeruginosa*	S. typhi	*C. albicans*
Pyrazoline[a]	+	+	+	+	+	+	–
Standard[b]	++	+++	+++	+++	+++	+++	+++
1	+++	++++	+++	++	+++	++	++
5	+++	+++	++++	+++	++++	+++	++

Inhibition values beyond control are + = 6–10, ++ = 11–15, +++ = 16–20, and ++++ = 21–25 mm (values include disc diameter). No activity was seen for *C. freundii*, *V. parahaemolyticus*, and *E. coli*.

[a] 3(2′-Hydroxyphenyl)-5-phenyl pyrazoline.

[b] The standards are in the form of sterile Hi-Disc cartridges, each disc containing 30 µm of the drug, terbinafin (antifungal agent) and chloramphenicol (antibacterial agent).

4. Conclusion

This study describes a series of the complexes of the type $[Fe(OCH_2CH_2O)(C_{15}H_{12}N_2OX)]_m \cdot nH_2O$ and $[Fe(C_{15}H_{12}N_2OX)_2(OCH_2CH_2OH)]$.

In $[Fe(OCH_2CH_2O)(C_{15}H_{12}N_2OX)]_m \cdot nH_2O$, pyrazoline and ethylene glycol are bidentate. TGA analysis shows coordinated water. Elemental analysis, molecular weight measurement, and FAB mass spectra reveal dimers or trimers. Electronic spectra indicate square pyramidal geometry around iron(III) [24, 25]; magnetic moments and molar conductivity measurements suggest high-spin non-electrolytes.

In $[Fe(C_{15}H_{12}N_2OX)_2(OCH_2CH_2OH)]$, pyrazoline and ethylene glycol are bidentate. elemental analysis, molecular weight measurement, and fab mass spectra reveal monomers. electronic spectral data indicate octahedral geometry around iron(III) [16, 21–23]. Magnetic moment studies and molar conductivity measurements suggest high-spin non-electrolytes. The complexes exhibit higher antibacterial and antifungal activity than the free pyrazoline, chloramphenicol, and terbinafin, respectively [28–31].

Acknowledgments

The authors are grateful to SAIF, CDRI, Lucknow, India; Punjab University, Chandigarh, India; IIT, Mumbai, India; SIF, IISc, Bangalore, India; APS University, Rewa, India; Inter University Consortium for the Department of Atomic Energy Facilities (DAEF), Indore, India; and USIC, Delhi University, New Delhi, India, for providing the necessary spectral and analytical data.

References

[1] J.R. Shah, N.R. Shah. *Indian J. Chem.*, **21A**, 312 (1982).
[2] J.R. Shah, S.K. Das, R.P. Patel. *J. Indian Chem. Soc.*, **50**, 228 (1973).
[3] N.R. Shah, J.R. Shah. *J. Inorg. Nucl. Chem.*, **43**, 1593 (1981).
[4] U.N. Tripathi, K.V. Sharma, A. Chaturvedi, T.C. Sharma. *Pol. J. Chem.*, **77**, 109 (2003).

[5] U.N. Tripathi, G. Vanubabu, Mohd. Safi Ahmad, S.S. Rao Kolisetty, A.K. Srivastav. *J. Appl. Organomet. Chem.*, **20**, 669 (2006).
[6] U.N. Tripathi, Mohd. Safi Ahmad, G. Venubabu, D.R. Khate. *Main Group Met. Chem.*, **29**, 39 (2006).
[7] U.N. Tripathi, Mohd. Safi Ahmad, G. Venubabu, P. Ramakrishna. *J. Coord. Chem.*, **60**, 1777 (2007).
[8] U.N. Tripathi, Mohd. Safi Ahmad, G. Venubabu, P. Ramkrishna. *J. Coord. Chem.*, **60**, 1709 (2007).
[9] U.N. Tripathi, Mohd. Safi Ahmad, G. Venubabu. *Turk J. Chem.*, **31**, 45 (2007).
[10] U.N. Tripathi, J.S. Solanki, A. Bhardwaj, T.R. Thapak. *J. Coord. Chem.*, **61**, 4025 (2008).
[11] U.N. Tripathi, J.S. Solanki, Mohd. Safi Ahmad, A. Bhardwaj. *J. Coord. Chem.*, **62**, 636 (2009).
[12] R. Gomer, G.N. Tyson. *J. Am. Chem. Soc.*, **66**, 1331 (1944).
[13] D. Knetsch, V.L. Groeneveld. *Inorg. Chim. Acta*, **7**, 81 (1973).
[14] D. Knetsch. *Diols as Lligands*, Rijk University, Leiden (1976).
[15] L. Labadi, G. Liptay, A. Horvath, L. Korecz, S. Papp, K. Burger. *J. Therm. Anal.*, **32**, 1575 (1987).
[16] U.N. Tripathi, K.V. Sharma, V. Sharma. *J. Coord. Chem.*, **61**, 3314 (2008).
[17] A.I. Vogel. *A Text Book of Quantitative Organic Analysis*, ELBS and Longman Group Ltd, London (1978).
[18] T.C. Sharma, V. Saxena, N.J. Readdy. *J. Acta Chim.*, **93**, 4 (1977).
[19] A.I. Vogel. *A Text Book of Quantitative Inorganic Analysis*, ELBS and Longman Group Ltd, London (1985).
[20] J.H. Benson. *Microbiological Application*, 5th Edn, Wm.C. Brown Publication, Oxford (1990).
[21] M. Revanasiddappa, T. Suresh, S. Khasim, S.C. Raghavendra, C. Basavaraja, S.D. Angadi. *E-J. Chem.*, **5**(2), 395 (2008).
[22] N. Saha, D.K. Sau. *Transition Met. Chem.*, **30**, 532 (2005).
[23] U.N. Tripathi, G. Shrivastava, R.C. Mehrotra. *Transition Met. Chem.*, **19**, 564 (1994).
[24] A.B.P. Lever. *Inorganic Electronic Spectroscopy*, Elsevier, Amsterdam (1968).
[25] D.P. Singh, R. Kumar. *J. Serb. Chem. Soc.*, **72**, 1069 (2007).
[26] R.M. Silverstein, F.X. Webster. *Spectrometric Identification of Organic Compounds*, 6th Edn, John Wiley & Sons Inc., New York (1998).
[27] K. Nakamoto. *Infrared and Raman Spectra of Inorganic and Coordination Compounds*, Wiley Interscience, New York (1997).
[28] U.N. Tripathi, K.V. Sharma, V. Sharma, R.K. Dubey. *J. Coord. Chem.*, **62**, 493 (2009).
[29] U.N. Tripathi, K.V. Sharma, V. Sharma. *J. Coord. Chem.*, **62**, 506 (2009).
[30] U.N. Tripathi, K.V. Sharma, V. Sharma. *J. Coord. Chem.*, **62**, 676 (2009).
[31] U.N. Tripathi, K.V. Sharma, V. Sharma. *J. Coord. Chem.*, **62**, 1846 (2009).